Plant Physiology and Biochemistry 198 (2023) 107712

Contents lists available at ScienceDirect

Plant Physiology and Biochemistry

journal homepage: www.elsevier.com/locate/plaphy

Evaluation of the alkalinity stress tolerance of three *Brassica rapa* CAX1 TILLING mutants

Eloy Navarro-León [a,*], Angela Grazioso [b], Santiago Atero-Calvo [a], Juan José Rios [a], Sergio Esposito [b], Begoña Blasco [a]

[a] Department of Plant Physiology, Faculty of Sciences, University of Granada, 18071, Granada, Spain
[b] Dipartimento di Biologia, Università di Napoli "Federico II", Complesso Universitario di Monte Sant'Angelo, Via Cinthia, 80126, Napoli, Italy

ARTICLE INFO

Handling Editor: K Kees Venema

Keywords:
Brassica rapa
$CaCO_3$
Mineral elements
Oxidative stress
Photosynthesis
TILLING

ABSTRACT

Alkalinity is an important environmental factor that affects crop production and will be exacerbated in the current climate change scenario. Thus, the presence of carbonates and high pH in soils negatively impacts nutrient assimilation and photosynthesis and causes oxidative stress. A potential strategy to improve tolerance to alkalinity could be the modification of cation exchanger (CAX) activity, given that these transporters are involved in calcium (Ca^{2+}) signaling under stresses. In this study, we used three *Brassica rapa* mutants (*BraA.cax1a-4, BraA.cax1a-7,* and *BraA.cax1a-12*) from the parental line 'R-o-18' that were generated by Targeting Induced Local Lesions in Genomes (TILLING) and grown under control and alkaline conditions. The objective was to assess the tolerance of these mutants to alkalinity stress. Biomass, nutrient accumulation, oxidative stress, and photosynthesis parameters were analyzed. The results showed that *BraA.cax1a-7* mutation was negative for alkalinity tolerance because it reduced plant biomass, increased oxidative stress, partially inhibited antioxidant response, and lowered photosynthesis performance. Conversely, the *BraA.cax1a-12* mutation increased plant biomass and Ca^{2+} accumulation, reduced oxidative stress, and improved antioxidant response and photosynthesis performance. Hence, this study identifies *BraA.cax1a-12* as a useful CAX1 mutation to enhance the tolerance of plants grown under alkaline conditions.

1. Introduction

Currently, agriculture is facing an increasing demand for food due to a constantly growing population. As a result, it is estimated that agricultural crop production needs to increase from 25% to 70% in the coming years (Hunter et al., 2017). In addition, the consequences of climate change continue to worsen each year with sudden events such as drought, floods, and high temperatures that seriously threaten yields. Furthermore, the increase in arid areas, soils with high salinity, and alkalinity levels due to high temperatures and drought exacerbates this problem. Therefore, it is urgent to identify measures to improve agricultural production and food quality in this critical scenario (Owino et al., 2022).

Specifically, alkaline and calcareous soils currently make up an important percentage of cultivable areas, especially in the Mediterranean area (Uzuner and Dengiz, 2020). These soils have high levels of $CaCO_3$ and HCO_3^- and a high pH. Alkalinity is a significant constraint for plant growth and crop productivity (Fatima et al., 2021; Rouphael et al., 2010; Yin et al., 2019). The negative effects are caused by osmotic stress, ion toxicity, and the direct impact of high pH in the growth media (Yin et al., 2019). Indeed, $CaCO_3$ is the compound with the greatest capacity to hinder pH reduction. Hence, soils with high $CaCO_3$ presence presented pH values higher than 7, making the bioavailability of most essential elements difficult (Tamir et al., 2021). Moreover, in these soils, bicarbonate ions interfere with the assimilation of nutrients, especially of P, K, and Mg, and reduce the availability of various micronutrients, mainly Fe (Capula-Rodríguez et al., 2016; Valdez-Aguilar and Reed, 2007). This fact is because there is a high rate of Fe^{3+} precipitation, which forms hydroxides or other non-soluble compounds (Taalab et al., 2019). Fe deficiency negatively affects plant physiology and biochemistry because it is a necessary cofactor of numerous enzymes, including those that participate in chlorophyll biosynthesis. Furthermore, iron is important for the formation of the chlorophyll's heme group, and its reduction causes a diminution of chlorophyll content and an impairment in the photosynthesis process (Huang and Wu, 2017). Thus,

* Corresponding author.
E-mail addresses: enleon@ugr.es (E. Navarro-León), angela.grazioso@unina.it (A. Grazioso), satero@ugr.es (S. Atero-Calvo), jjrios@ugr.es (J.J. Rios), sergio.esposito@unina.it (S. Esposito), bblasco@ugr.es (B. Blasco).

https://doi.org/10.1016/j.plaphy.2023.107712
Received 12 February 2023; Received in revised form 13 April 2023; Accepted 17 April 2023
Available online 18 April 2023

Abbreviations

A	net photosynthesis rate
APX	ascorbate peroxidase
ASA	ascorbate
E	transpiration rate
GSH	glutathione
CAX	cation exchangers
DHA	dehydroascorbate
EL	electrolyte leakage
GR	glutathione reductase
g_s	stomatal conductance
GSSG	oxidized glutathione
MDA	malondialdehyde
PAR	photosynthetic active radiation
PS	photosystem
RC	reaction center
SOD	superoxide dismutase
TILLING	Targeting Induced Local Lesions in Genomes
WUE	water use efficiency

photosynthesis is a process highly affected by alkalinity in crops and is therefore a significant indicator of plant tolerance to it (Li et al., 2014; Wang et al., 2022; Yin et al., 2019).

Furthermore, another element that is significant in alkalinity is Ca^{2+}. High levels of this element are toxic to plants, inhibiting seed germination, reducing plant growth, and damaging cells because of the formation of Ca oxalate crystals (White and Broadley, 2003). Additionally, when its concentration is high, it induces prolonged stomatal closure, leading to a decrease in internal CO_2 and, as a result, photosynthesis. Ca^{2+} also regulates aquaporins like PIP, and an increase in its concentration reduces the activity of aquaporins (Dayod et al., 2010). Besides, Ca^{2+} excess is also an abiotic stress factor as it reduces photosynthetic efficiency by preventing the correct flow of electrons and promotes the generation of reactive oxygen species (ROS) (Bačkor et al., 2017). During oxidative stress, high-energy electrons are transferred to molecular oxygen producing ROS that are toxic compounds for plants. ROS cause disorganization of thylakoid structures, inhibit chlorophyll synthesis, and affect the functioning of photosystem II (D'Alessandro et al., 2013; Gururani et al., 2015). Likewise, ROS interfere with cell compounds such as membrane lipids, and nucleic acids, leading to lipid peroxidation or DNA mutations (Chakradhar et al., 2017).

In plant cells, cytosolic Ca^{2+} levels are mainly regulated by cation exchanger (CAX) transporters that participate in the transfer of bivalent cations such as Ca^{2+} into cell vacuoles. CAXs are essential for the maintenance of cellular homeostasis to produce the necessary concentration changes in cell signaling and respond to environmental signals (Conn et al., 2011). Several experiments proved that modifying CAX transporters or their gene expression levels can be useful for stress tolerance in numerous species (Ahmadi et al., 2018; Pittman and Hirschi, 2016). In recent years, biotechnological techniques have been developed to produce new plant varieties adapted to adverse conditions, such as drought or salinity (Derbyshire et al., 2022). One of these techniques is Targeting Induced Local Lesions in Genomes (TILLING), which involves the generation of random mutations, identifying variations in specific sequences, and associating them with a function or phenotype, allowing the identification of mutants without the need for transgenic breeding (Till et al., 2018). Using TILLING, the expression levels and substrate specificity of the CAX1 transporter were modified. These modifications resulted from single amino acid changes in the N-terminal regulatory region of CAX1 (Lochlainn et al., 2011; Manohar et al., 2011). Thus, studies were carried out in these TILLING mutants and they revealed improvements in facing various abiotic stresses, including salinity (Navarro-León et al., 2020a, 2020b). Furthermore, certain CAX1 modifications improve nutrient accumulation, photosynthesis performance, and ROS detoxification through ascorbate/glutathione (AsA/GSH) cycle enhancement (Navarro-León et al., 2020; Navarro-León et al., 2018). Therefore, in the present study, we aim to determine whether these CAX1 mutations confer tolerance to plants grown under alkaline conditions with high $CaCO_3$ in the growth media, by analyzing growth, nutrient accumulation, photosynthesis, antioxidant response, and photosynthesis performance.

2. Material and methods

2.1. Plant material and growth conditions

Three *B. rapa* ssp. trilocularis 'R-o-18' mutants were used: *BraA.cax1a-4* (Alanine-to-Threonine change at amino acid 77), *BraA.cax1a-7* (Arginine-to-Lysine change at amino acid 44), and *BraA.cax1a-12* (Proline-to-Serine change at amino acid 56) and the parent line (R-o-18). The mutants were produced by TILLING technique as detailed by Lochlainn et al. (2011) and Graham et al. (2014). *B. rapa* seeds were placed on filter paper in Petri dishes until germination and then put in pots (13 cm × 13 cm x 12.5 cm) filled with vermiculite that were arranged in plastic trays (55 cm × 40 cm x 8.5 cm) and placed in a growth chamber. The environmentally controlled conditions were: temperature (22/18 °C; day/night), humidity (60–80%), photoperiod (14/10-h; day/night), and photosynthetic active radiation (PAR) (350 μmol m-2 s-1). The plants were supplied with a Hoagland nutritive solution composed of 6 mM KH_2PO_4, 4 mM $Ca(NO_3)_2 \bullet 4\ H_2O$, 4 mM KNO_3, 2 mM $MgSO_4 \bullet 7\ H_2O$, 1 mM $NaH_2PO_4 \bullet 2\ H_2O$, 10 μM H_3BO_3, 5 μM Fe-chelate (Sequestrene; 138 FeG100), 2 μM $MnCl_2 \bullet 4\ H_2O$, 1 μM $ZnSO_4$, 0.25 μM $CuSO_4 \bullet 5\ H_2O$, and 0.1 μM $Na_2MoO_4 \bullet 2\ H_2O$. The pH of this solution was 5.5–6.0. The solution in the trays was removed every three days to prevent salt accumulation. For this, the trays were carefully washed with distilled water, and new nutritive solution was added.

2.2. Experimental design and treatments

The treatments were applied 30 days after germination and were maintained for 21 days. There were two different treatments: the control and the alkalinity treatment. Plants of the control treatment were watered with the previously described nutritive solution, while plants of the alkalinity treatment were watered with the same nutritive solution plus the addition of 25 mM $^{CaCO}_{3}$ and a pH of 7.5–8.0. The trial involved two factors: alkalinity and *BraA.cax1a* mutation ('R-o-18', *BraA.cax1a-4*, *BraA.cax1a-7*, and *BraA.cax1a-*$^{12)}$. The experimental design consisted of a randomized complete block with 8 plants per tray and 3 trays (replications) per treatment, resulting in a sample size of 24 plants per treatment. Plant material was collected from each plant of each treatment and homogenized to obtain representative samples.

2.3. Plant sampling

The shoots were cut, washed with distilled water, and then dried on filter paper and weighed to determine the fresh weight (FW). A part of the plant material was lyophilized to obtain the dry weight (DW) and determine the concentrations of mineral elements, and the other part was frozen at −40 °C for use in biochemical analysis.

2.4. Plant material analysis

2.4.1. Relative growth rate

To measure the relative growth rate, leaves from each treatment were taken before the application of alkalinity. These leaves were dried in an oven at 70 °C for 24 h, and then weighed to obtain the initial dry weight (DW_i). At the end of the experiment, the final dry weight (DW_f) of the plants was obtained. The relative growth rate value was calculated

using the equation RGR = (ln DWi – ln DWf)/T). T = 21 days.

2.4.2. Nutrient concentration

Leaf samples were ground and mineralized through wet digestion (Wolf, 1982). 0.1 g of leaves were taken and mineralized using nitric acid (HNO_3) and 30% hydrogen peroxide (H_2O_2). After mineralization, 20 mL of distilled water was added, and the concentration of mineral elements most affected by the presence of alkaline stress (K^+, Ca^{2+}, Mg^{2+}, Fe^{3+}, Cu^{2+}, Mn^{2+} and Zn^{2+}) were determined through spectrometric techniques (IPC-OES).

2.4.3. Cell membrane stability

The determination of cell membrane stability was carried out using the electrolyte leakage test described by Soloklui et al. (2012). For this purpose, eight pieces of leaves obtained from different plants were cut, gently washed with deionized water, and placed in a Falcon tube containing 30 mL of deionized water. The tubes were then vortexed for 1 min and the initial conductivity (EC_1) was measured using a conductivity meter (Cond 8; XS Instruments, Italy). The samples were then kept at 100 °C for 20 min to extract the released electrolytes and allowed to cool to room temperature. Finally, the final conductivity (EC_2) was measured, and the percentage of electrolyte leakage was determined using the formula: (EC1/EC2) x 100.

2.4.4. Determination of oxidative stress indicators

Malondialdehyde (MDA) concentration was measured by spectrophotometry as described by Fu and Huang (2001). The method described by Junglee et al. (2014) was used to determine H_2O_2 concentration. The $O_2^{\bullet-}$ concentration was determined according to Xiao et al. (1999) by spectrophotometry.

2.4.5. Determination of antioxidant enzyme activities

Superoxide dismutase (SOD) activity was measured as described by Yu et al. (1998). This method is based on the inhibition of the photochemical reduction of nitroblue tetrazolium (NBT). The plant material (0.1 g) was extracted with 50 mM Hepes-HCl Buffer (pH 7.6). Subsequently, it was centrifuged at 11000 rpm for 10 min. For the reaction, 5 μl of the resulting supranatant containing SOD enzyme were mixed with the 195 μl of the reaction buffer containing 50 mM Na_2CO_3 (pH10.2), 12 mM methionine, 0.1 mM EDTA-Na, 75 μM NBT, and 15 μM riboflavin. The was placed in a microplate, was illuminated for 15 min at a PPFD of 380 $\mu mol^{-2}s^{-1}$, and the absorbance was read at 650 nm. Some replications of the samples were not illuminated to correct background absorbance. One unit of SOD activity was defined as the amount of enzyme required to cause 50% inhibition of NBT reduction.

The methodology described by Rao et al. (1996) was used to determine ascorbate peroxidase (APX) and glutathione reductase (GR) enzyme activities. The plant material (0,1 g) was extracted with 100 mM phosphate potassium buffer (pH 7.5) and 0,05 mM EDTA-Na and was centrifuged at 12000 rpm for 20 min. The obtained supernatant was used for the APX and GR reactions. For APX, 40 μl of the extract was mixed with 80 μl of 100 mM phosphate potassium buffer (pH 7.5), 40 μl of 0.5 mM ascorbate, and 40 μl of 0.2 mM H_2O_2. The decrease in absorbance due to H_2O_2 consumption was measured at 290 nm for 3 min. For GR activity determination 30 μl of the previously obtained extract was mixed with 90 μl of 100 mM Tris-HCl (pH 7.8), 40 μl of 0.2 mM NADPH, and 40 μl of 0.5 mM GSSG. Then, the oxidation of NADPH at 340 nm was registered for 3 min. Enzyme activity was expressed as ΔAbs min^{-1} mg^{-1} protein. Protein concentration was quantified using the Bradford method (Bradford, 1976).

2.4.6. Determination of ascorbic acid (AsA) and glutathione (GSH) concentrations

The method described by Law et al. (1983) was used to quantify total AsA and reduced AsA concentrations. The dehydroascorbate (DHA) concentration was calculated by subtracting the concentration of reduced AsA from that of total AsA. The methodology described by Noctor and Foyer (1998) was followed to determine oxidized GSH (GSSG), and total GSH (reduced GSH + GSSG). The reduced GSH concentration was calculated by subtracting the concentration of GSSG from that of the total GSH. The next formula: [(Reduced form) X 100]/[Reduced + Oxidized forms] was used to calculate AsA and GSH redox states.

2.5. Fluorescence parameters

The Handy PEA Chlorophyll Fluorimeter (Hansatech Ltd., King's Lynn, Norfolk, UK was used to obtain Chl *a* fluorescence parameters. The analysis was performed on developed and intermediate leaves of nine intact plants per treatment. The measurement area in leaves was kept in darkness for 30 min utilizing leaf clip holders. The fluorescence transients with OJIP phases were induced by red light (650 nm; 3000 μmol photons $m^{-2}s^{-1}$). The obtained parameters were: fluorescence origin (Fo), fluorescence maximum (F_M), variable Fluorescence (F_M-Fo = F_V), maximum quantum yield of primary photosystem II (PSII) photochemistry (F_V/F_M), standardized area above the fluorescence curve (S_m), the proportion of active reaction centers (RC) (RC/ABS), dissipated energy flux per RC at t = 0 (DI_o/RC), fluorescence value at 300 μs (K step), efficiency with which a trapped exciton move an electron further than quinone A into the electron transport chain (ψ_o), quantum yield for electron transport from quinone A to plastoquinone (φ_{Eo}), the probability that PSII Chl molecule function as RC (γ_{RC}), the performance index of electron flux from PSII based to intersystem acceptors (PI_{ABS}), and performance index of electron flux to PSI electron acceptors (PI_{total}) (Strasser et al., 2000). To represent these parameters the mean of each different *BraA.cax1a* plant was divided by the mean of R-o-18 plants grown under alkalinity conditions for each parameter to normalize the data and enable the comparison of parameters of different scales.

2.6. Gas exchange parameters

An infra-red gas analyzer LICOR 6800 Portable Photosynthesis System (IRGA: LICOR Inc. Nebraska, USA) was used. The fully developed leaves of nine intact plants for each treatment were positioned in the leaf cuvette set with optimal growth conditions. The device was warmed up for 30 min and calibrated prior to the measurements. The cuvette conditions were: 60% relative humidity, 350 μmol m^2 s^{-1} PAR, and 500 μmol mol^{-1} CO_2 concentration. Net photosynthesis rate (*A*), transpiration rate (*E*), and stomatal conductance (g_s) were obtained. Instantaneous water use efficiency (WUE) was determined by dividing *A* by the corresponding *E*.

2.7. Statistical analysis

The statistical analysis was conducted using Statgraphics Centurion XVI software. The data underwent a simple analysis of variance (ANOVA), and a multifactorial ANOVA test was performed to assess the effects of the application and alkalinity on the mutant (A x M) and their significant influence on the results. The means were compared using Fisher's least significant differences (LSD). The significance levels for both analyses were denoted as follows: * for $P < 0.05$, ** for $P < 0.01$, *** for $P < 0.001$, and NS for not significant.

3. Results

3.1. Weight and relative growth rate

The application of alkaline stress to *B. rapa* plants decreased leaf biomass compared to control plants, except in *BraA.cax1a-12* plants where no significant differences were observed. When comparing the different genotypes grown under control conditions, it was observed that the mutant plants had lower DW, FW, and RGR than the R-o-18

plants, with *BraA.cax1a-7* having the lowest biomass. *BraA.cax1a-12* showed higher values than the other genotypes. On the other hand, *BraA.cax1a-7* was the mutant with the lowest biomass values (Table 1).

3.2. Mineral elements concentration

BraA.cax1a-4 and *BraA.cax1a-7* mutations enhanced K^+ accumulation, while all mutations increased Ca^{2+} accumulation and did not cause effects on Mg^{2+} concentration in *B. rapa* grown under control conditions. Alkaline stress reduced K^+ levels, increased Ca^{2+}, and did not affect Mg^{2+} accumulation, except in *BraA.cax1a-12* with no variations in these elements compared to control conditions (Table 2). Under alkaline conditions, *BraA.cax1a-4* and *BraA.cax1a-7* mutants showed higher K^+ and lower Mg^{2+} concentrations, while *BraA.cax1a-12* presented higher Ca^{2+} accumulations compared to R-o-18 plants (Table 2).

Regarding micronutrients, *BraA.cax1a-4* registered higher Fe^{3+} and Zn^{2+} levels, while *BraA.cax1a-7* showed greater Mn^{2+} and Cu^{2+} than R-o-18 plants under control conditions. Generally, alkalinity reduced micronutrient accumulation in *B. rapa* plants, with the exceptions of Fe^{3+}, Mn^{2+}, and Cu^{2+} accumulation in *BraA.cax1a-12*, and Mn^{2+} and Cu^{2+} in *BraA.cax1a-4* plants, which maintained control levels of these elements under alkaline conditions (Table 3). All *BraA.cax1a* plants showed higher Mn^{2+} concentrations under alkaline conditions compared to R-o-18 plants (Table 3). Regarding the other analyzed micronutrients, *BraA.cax1a-4* plants registered higher values than R-o-18 plants (Table 3).

3.3. Electrolyte leakage, malondialdehyde, and ROS concentrations

BraA.cax1a-7 plants grown under control conditions showed higher EL percentage and $O_2^{\bullet-}$ levels, but *BraA.cax1a-12* presented lower MDA concentration than R-o-18 plants. Furthermore, the results showed an increase in oxidative stress indicators in *B. rapa* plants subjected to alkaline stress compared to control conditions, with the exception of EL and H_2O_2, which did not increase significatively in *BraA.cax1a-12* plants (Table 4). When comparing *B. rapa* genotypes grown under alkaline stress, mutant *BraA.cax1a-7* presented the highest EL and H_2O_2 values.

Table 1
Effect of alkalinity and *BraA.cax1a* mutations on shoot biomass and RGR in *B. rapa* plants.

		Fresh weight	Dry weight	RGR
		g plant^{-1}	g plant^{-1}	
Control	R-o-18	0.70 ± 0.06a	10.61 ± 1.47a	0.106 ± 0.006c
	BraA.cax1a-4	0.65 ± 0.09a	10.17 ± 1.68a	0.115 ± 0.008ab
	BraA.cax1a-7	0.52 ± 0.09 b	7.90 ± 1.17b	0.112 ± 0.007bc
	BraA.cax1a-12	0.64 ± 0.09a	9.57 ± 0.42ab	0.120 ± 0.002a
	p-value	*	*	*
	$^{LSD}0.05$	0.11	1.7	0.008
Alkalinity	R-o-18	0.56 ± 0.04b	8.14 ± 0.62b	0.093 ± 0.003c
	BraA.cax1a-4	0.54 ± 0.08b	7.92 ± 1.68b	0.104 ± 0.007b
	BraA.cax1a-7	0.31 ± 0.04c	4.34 ± 0.59c	0.083 ± 0.006d
	BraA.cax1a-12	0.65 ± 0.04a	9.51 ± 0.60a	0.120 ± 0.003a
	p-value	***	***	***
	$^{LSD}0.05$	0.07	1.08	0.007
Analysis of variance				
Alkalinity (A)		***	***	***
Mutation (M)		***	***	***
A x M		*	**	***
$^{LSD}0.05$		0.04	0.69	0.004

Values are means ± standard deviation (n = 9). The levels of significance were represented as * ($p < 0.05$), ** ($p < 0.01$), and *** ($p < 0.001$). Values with different letters indicate significant differences.

Table 2
Effect of alkalinity and *BraA.cax1a* mutations on cationic macronutrients concentration in *B. rapa* plants.

		K^+	Ca^{2+}	Mg^{2+}
		mg g^{-1} DW	mg g^{-1} DW	mg g^{-1} DW
Control	R-o-18	58.43 ± 1.60 b	21.03 ± 0.09c	10.64 ± 0.69a
	BraA.cax1a-4	68.10 ± 6.56a	23.31 ± 0.74b	9.49 ± 0.31a
	BraA.cax1a-7	68.47 ± 4.63a	23.96 ± 0.60b	9.52 ± 0.13a
	BraA.cax1a-12	53.59 ± 3.80b	28.43 ± 0.75a	10.94 ± 1.33a
	p-value	**	***	NS
	$^{LSD}0.05$	8.50	1.15	1.45
Alkalinity	R-o-18	50.40 ± 1.81b	26.41 ± 0.72b	10.12 ± 0.20a
	BraA.cax1a-4	61.90 ± 1.44a	26.36 ± 0.45b	9.40 ± 0.16b
	BraA.cax1a-7	62.90 ± 3.40a	27.18 ± 0.65ab	9.31 ± 0.18b
	BraA.cax1a-12	52.61 ± 1.95b	28.54 ± 1.12a	10.62 ± 0.63a
	p-value	***	*	**
	$^{LSD}0.05$	4.29	1.46	0.66
Analysis of variance				
Alkalinity (A)		**	***	NS
Mutation (M)		***	***	**
A x M		NS	***	NS
$^{LSD}0.05$		3.10	0.60	0.52

Values are means ± standard deviation (n = 9). The levels of significance were represented as NS ($p > 0.05$), * ($p < 0.05$), ** ($p < 0.01$), and *** ($p < 0.001$). Values with different letters indicate significant differences.

Table 3
Effect of alkalinity and *BraA.cax1a* mutations on micronutrients concentration in *B. rapa* plants.

		Fe^{3+}	Mn^{2+}	Zn^{2+}	Cu^{2+}
		μg g^{-1} DW	μg g^{-1} DW	μg g^{-1} DW	μg g^{-1} DW
Control	R-o-18	144.43 ± 9.05 b	90.70 ± 4.11 b	50.60 ± 5.93bc	18.32 ± 0.71bc
	BraA. cax1a-4	267.82 ± 17.48a	93.44 ± 3.95 b	65.04 ± 3.57a	20.71 ± 1.98 b
	BraA. cax1a-7	169.05 ± 15.94 b	114.55 ± 4.69a	51.38 ± 1.90 b	24.52 ± 1.27a
	BraA. cax1a-12	132.59 ± 20.40 b	93.54 ± 10.04 b	44.12 ± 1.50c	17.74 ± 1.06c
	p-value	***	**	***	**
	$^{LSD}0.05$	37.25	11.73	6.90	2.52
Alkalinity	R-o-18	126.94 ± 0.87 b	82.71 ± 1.70 b	47.21 ± 0.85 b	16.13 ± 0.58 b
	BraA. cax1a-4	157.76 ± 0.35a	90.60 ± 1.20a	52.47 ± 3.39a	21.24 ± 1.15a
	BraA. cax1a-7	138.22 ± 9.17 ab	95.78 ± 5.19a	39.07 ± 2.87c	17.04 ± 0.98 b
	BraA. cax1a-12	130.58 ± 22.56 b	90.34 ± 5.07a	40.02 ± 1.02c	17.20 ± 1.14 b
	p-value	*	*	***	**
	$^{LSD}0.05$	22.94	7.11	4.37	1.86
Analysis of variance					
Alkalinity (A)		***	**	***	***
Mutation (M)		***	***	***	***
A x M		***	NS	*	***
$^{LSD}0.05$		20.11	6.31	3.04	1.44

Values are means ± standard deviation (n = 9). The levels of significance were represented as NS ($p > 0.05$), * ($p < 0.05$), ** ($p < 0.01$), and *** ($p < 0.001$). Values with different letters indicate significant differences.

Table 4
Effect of alkalinity and *BraA.cax1a* mutations on oxidative stress indicators in *B. rapa* plants.

		EL (%)	MDA (μM g^{-1} FW)	$O_2^{\bullet-}$ (μg g^{-1} FW)	H_2O_2 (μg g^{-1} FW)
Control	R-o-18	19.98 ± 1.15 b	2.98 ± 0.42a	3.48 ± 0.11 b	28.20 ± 1.53a
	BraA. cax1a-4	19.10 ± 2.32 b	2.85 ± 0.26a	3.34 ± 0.17 b	25.08 ± 1.75a
	BraA. cax1a-7	22.11 ± 0.03a	3.10 ± 0.11a	3.63 ± 0.11a	27.71 ± 2.76a
	BraA. cax1a-12	20.48 ± 0.29 b	2.41 ± 0.15 b	3.33 ± 0.10 b	20.56 ± 2.38a
	p-value	***	**	**	NS
	$LSD_{0.05}$	1.10	0.31	0.15	6.37
Alkalinity	R-o-18	22.89 ± 1.39 b	4.12 ± 0.21 ab	4.23 ± 0.25a	38.84 ± 2.67 b
	BraA. cax1a-4	21.15 ± 1.22 b	4.32 ± 0.24a	3.81 ± 0.05 b	32.99 ± 2.23 b
	BraA. cax1a-7	37.08 ± 3.77a	4.00 ± 0.12 b	3.88 ± 0.10 b	58.55 ± 2.63a
	BraA. cax1a-12	20.73 ± 0.83 b	2.78 ± 0.14c	3.62 ± 0.14c	20.63 ± 1.11c
	p-value	***	***	***	***
	$LSD_{0.05}$	3.90	0.22	0.18	6.63
Analysis of variance					
Alkalinity (A)		***	***	***	***
Mutation (M)		***	***	***	***
A x M		***	***	***	***
$LSD_{0.05}$		1.87	0.19	0.11	4.45

Values are means ± standard deviation (n = 9). The levels of significance were represented as NS ($p > 0.05$), ** ($p < 0.01$), and *** ($p < 0.001$). Values with different letters indicate significant differences.

Conversely, mutation *BraA.cax1a-12* reduced MDA, $O_2^{\bullet-}$, and H_2O_2 values compared to R-o-18 plants (Table 4).

Consideration of AsA/GSH cycle parameters showed that under alkalinity conditions, the three *BraA.cax1a* mutants had greater SOD activity compared to R-o-18 plants, with the highest values found in the *BraA.cax1a-7* mutant (Fig. 1; Table S1). With regard to APX activity, it was lower in *BraA.cax1a-7* and greater in *BraA.cax1a-4* and *BraA.cax1a-12* plants compared to R-o-18 plants (Fig. 1; Table S1). In addition, *BraA.cax1a-7* plants presented lower reduced AsA and higher DHA levels, resulting in a lower AsA redox state. Alternatively, *BraA.cax1a-12* plants registered lower DHA concentrations, but their AsA redox state was not different from that of R-o-18 plants (Fig. 1; Table S2). Concerning GSH, a lower GR activity was observed in *BraA.cax1a-7*, whereas this enzyme showed enhanced activity in *BraA.cax1a-4* and *BraA.cax1a-12* plants compared to R-o-18 plants. The GSH redox state was increased by *BraA.cax1a-7* and *BraA.cax1a-12* mutations because of an increase in reduced GSH levels and a reduction in GSSG concentration compared to R-o-18 plants (Fig. 1; Table S3).

3.4. Photosynthesis performance

The analysis of Chl *a* fluorescence kinetics in our four genotypes subjected to alkalinity revealed the four typical OJIP phases (Fig. 2A). In Fig. 2A, *BraA.cax1a-7* is identified as the one that presented the highest fluorescence values in all OJIP phases. In contrast, mutants *BraA.cax1a-4* and *BraA.cax1a-12* showed slightly higher values than the parental R-o-18 in the O phase, while in the P phase, the fluorescence was lower in these mutants. Moreover, the analysis of parameters derived from de OJIP data showed that *BraA.cax1a-7* presented higher values of Fo, F_M, DI_o/RC, and K step but much lower values of F_V/F_M, RC/ABS, Ψ_o, Φ_{Eo}, γ_{RC}, and PI than the parental R-o-18 under alkalinity conditions (Fig. 2B). Conversely, the effects of *BraA.cax1a-12* mutation were generally positive since this mutant showed higher Sm, Ψ_o, PI_{ABS}, and PI_{total} compared to parental R-o-18 plants. Finally, *BraA.cax1a-4* showed higher DI_o/RC and lower RC/ABS and PI_{total} values, although the effect was not as important as that caused by *BraA.cax1a-7* (Fig. 2B).

The gas exchange results showed that *BraA.cax1a-7* plants registered lower *A* and WUE values than the other genotypes grown under control conditions. However, under these conditions, *BraA.cax1a-12* plants presented lower *E* and g_s but higher WUE values compared to the other plants. When alkaline conditions were applied, *A* and WUE were reduced compared to control conditions, except in the *BraA.cax1a-12* genotype. Furthermore, *E* and g_s were only reduced in R-o-18 under alkaline treatment compared to control conditions. Finally, when comparing genotypes grown under alkaline conditions, it was found that *BraA.cax1a-7* had lower *A* and WUE values. This mutant, together with *BraA.cax1a-4*, presented higher *E* and g_s values, while *BraA.cax1a-12* showed the greatest WUE index compared to the other genotypes (Table 5).

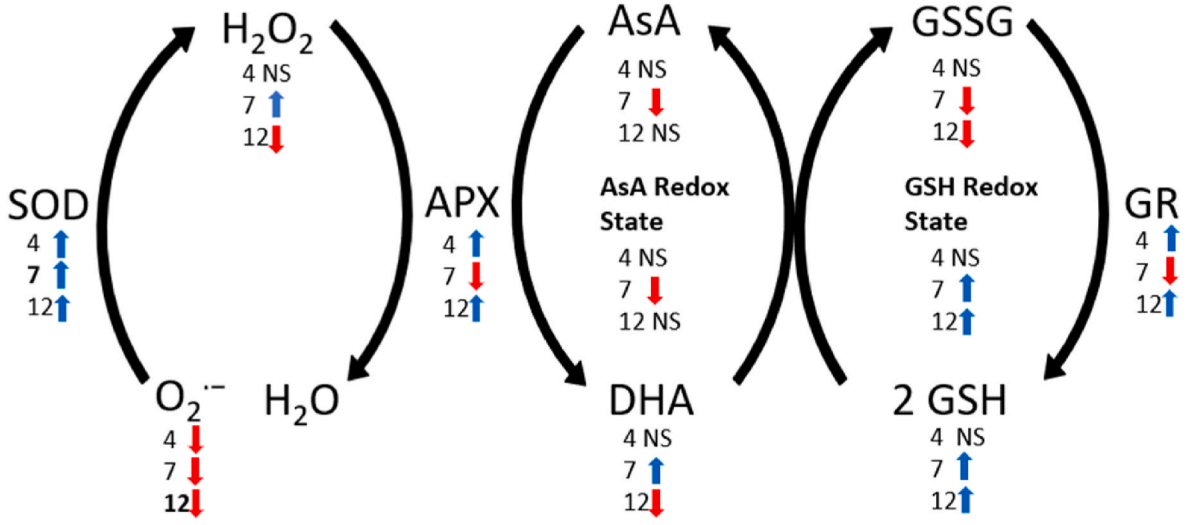

Fig. 1. Effect of *BraA.cax1a* mutations on antioxidant enzyme activities and AsA/GSH cycle in *B. rapa* plants grown under alkaline conditions. Blue arrows indicate increments and red arrows indicate reductions of these parameters compared to the values of R-o-18 plants. The genotype marked in bold is the one that showed the greatest increases or decreases with respect to R-o-18 plants.

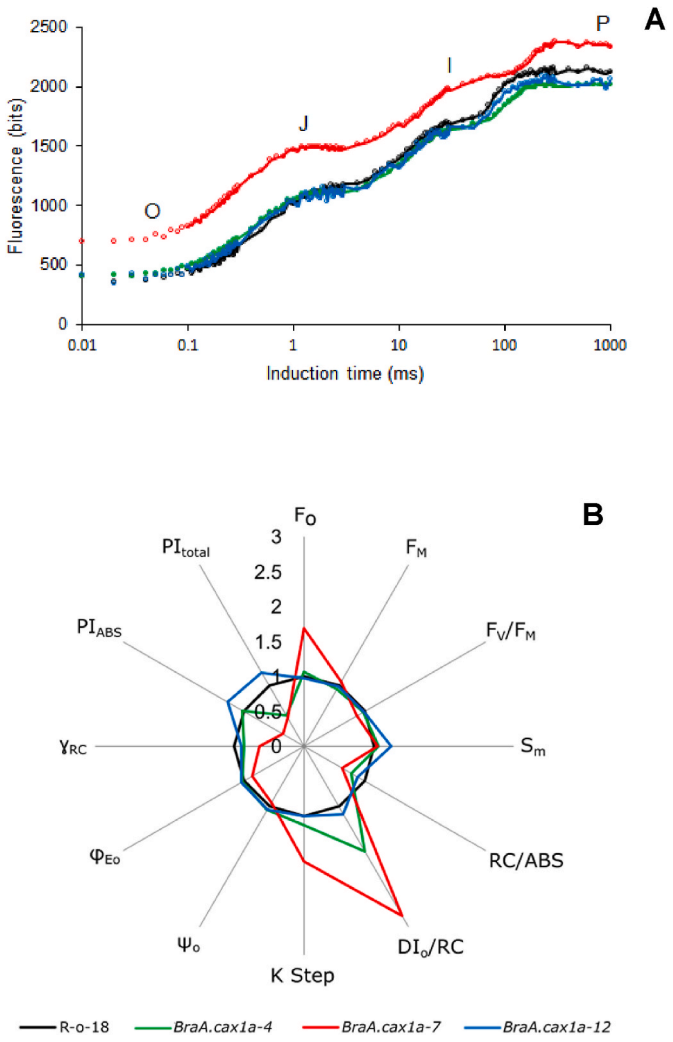

Fig. 2. Results from Chl *a* fluorescence analysis in *BraA.cax1a* and R-o-18 plants subjected to alkalinity. Native fluorescence induction curves (A). Radar plot showing OJIP-test parameters derived from Chl *a* fluorescence induction (B). Data normalization was made to enable the representation of all parameters on the same scale. The colored lines represent the relative increase or decrease in each of the *BraA.cax1a* mutants with respect to R-o-18 plants (black line). Represented values are means from nine data (n = 9).

4. Discussion

4.1. Plant growth

Several studies have shown that the primary effect of alkaline stress is a reduction in biomass. For instance, different species grown with elevated concentrations of $CaCO_3$ or other carbonates and high pH in the culture media presented lower growth rates (Cardarelli et al., 2010; de la Torre-González et al., 2018; Fatima et al., 2021; Tamir et al., 2021). In this study, the application of alkaline stress to *B. rapa* plants also decreased leaf biomass, except for *BraA.cax1a-12* plants, which exhibited better biomass indicators than the other genotypes. On the other hand, *BraA.cax1a-7* was the mutant with the lowest biomass values (Table 1). These findings suggest that CAX1 transporters influence the growth of plants grown under alkaline conditions and that the mutation in *BraA.cax1a-12* could enhance tolerance to high $CaCO_3$ concentrations.

Table 5
Effect of alkalinity and *BraA.cax1a* mutations on gas exchange parameters in *B. rapa* plants.

		A	*E*	g_s	WUE
		μmol m^{-2} s^{-1}	mmol m^{-2} s^{-1}	mol m^{-2} s^{-1}	mmol $mmol^{-1}$
Control	R-o-18	46.01 ± 2.14a	12.67 ± 0.74a	1.16 ± 0.08 b	3.63 ± 0.08 b
	BraA. cax1a-4	46.48 ± 3.26a	12.72 ± 1.18a	1.18 ± 0.14 ab	3.66 ± 0.08 b
	BraA. cax1a-7	36.02 ± 0.92 b	13.32 ± 0.51a	1.33 ± 0.05a	2.70 ± 0.05c
	BraA. cax1a-12	42.20 ± 4.98a	9.92 ± 1.68 b	0.96 ± 0.12c	4.28 ± 0.25a
	p-value	**	**	**	***
	$^{LSD}0.05$	4.92	1.73	0.16	0.22
Alkalinity	R-o-18	34.79 ± 5.34 ab	10.13 ± 1.35 b	0.88 ± 0.12 b	3.32 ± 0.20 b
	BraA. cax1a-4	38.41 ± 1.56a	12.92 ± 0.86a	1.23 ± 0.14a	2.98 ± 1.18 b
	BraA. cax1a-7	30.13 ± 2.37 b	13.11 ± 1.14a	1.24 ± 0.16a	2.30 ± 0.10c
	BraA. cax1a-12	38.49 ± 4.83a	9.42 ± 1.60 b	0.78 ± 0.14 b	4.12 ± 0.38a
	p-value	*	**	**	***
	$^{LSD}0.05$	5.96	1.95	0.22	0.36
Analysis of variance					
Alkalinity (A)		***	NS	*	***
Mutation (M)		***	***	***	***
A x M		NS	NS	NS	NS
$^{LSD}0.05$		2.59	0.87	0.09	0.14

Values are means ± standard deviation (n = 9). The levels of significance were represented as NS ($p > 0.05$), * ($p < 0.05$), ** ($p < 0.01$), and *** ($p < 0.001$). Values with different letters indicate significant differences.

4.2. Nutrient concentration

Previous studies proved that both CAX1 modifications and alkaline stress have an impact on the accumulation of mineral element in plants (Bessrour et al., 2018; Conn et al., 2011; de la Torre-González et al., 2018; Navarro-León et al., 2018). The reduction of K^+ and the increment in Ca^{2+} concentrations are common effects of alkaline stress when $CaCO_3$ is applied to other species (Bessrour et al., 2018; Cardarelli et al., 2010; Tamir et al., 2021). These variations in Ca^{2+} and K^+ accumulation were also observed in most of the analyzed genotypes in our study (Table 2). Other studies noted that an adequate supply of K^+ and Ca^{2+} can be beneficial in the tolerance to alkaline stress (Capula-Rodríguez et al., 2016; Wei et al., 2020). Hence, the higher Ca^{2+} accumulation of *BraA.cax1a-12* and the maintenance of cationic macronutrient concentrations could be key factors in the greater tolerance of this mutant to alkalinity.

In general, the effect of alkalinity on the accumulation of micronutrients in *B. rapa* plants was negative (Table 3). A decrease in micronutrient accumulation in growth media with high pH and the presence of carbonates is a common effect (Cardarelli et al., 2010; de la Torre-González et al., 2018; Rouphael et al., 2010). However, in some studies, an increment in Mn^{2+} concentration was observed (Bessrour et al., 2018; Tamir et al., 2021). This effect on Mn^{2+} accumulation may be enhanced by CAX1 modifications since all *BraA.cax1a* plants showed higher Mn^{2+} concentrations under alkaline conditions (Table 3). This result is supported by the fact that CAX1 can also transport Mn^{2+} into vacuoles facilitating its accumulation in the shoot (Conn et al., 2011). Regarding the rest of the analyzed micronutrients, *BraA.cax1a-4* plants registered higher values compared to R-o-18 plants (Table 3). Therefore, this mutation could promote the accumulation of micronutrients under alkaline stress conditions.

4.3. Oxidative stress indicators and antioxidant response

As in most stresses affecting plants, alkaline stress causes an accumulation of ROS and increased degradation of cell membranes, often leading to an increased in MDA generation and electrolyte leakage (EL) (de la Torre-González et al., 2018; Fatima et al., 2021; Montesinos-Pereira et al., 2018; Yin et al., 2019). In our experiment, the results showed an increment in oxidative stress indicators in *B. rapa* plants subjected to alkaline stress. Two exceptions were EL and H_2O_2, which did not significantly increase in *BraA.cax1a-12* plants (Table 4). Moreover, the results suggest that *BraA.cax1a-7* plants experienced higher oxidative stress than *BraA.cax1a-12* plants, indicating that the latter genotype is better adapted to alkaline stress.

Plants activate several defense mechanisms, including antioxidant enzyme activities and the accumulation of antioxidant compounds such as AsA and GSH, to cope with oxidative stress caused by alkalinity (de la Torre-González et al., 2018; Fatima et al., 2021; Liu and Saneoka, 2019; Yin et al., 2019). Overall, in our study, the results from the AsA-GSH cycle suggested a negative effect of the *BraA.cax1a-7* mutation on AsA regulation and a general enhancement of the cycle by *BraA.cax1a-12* mutation, which could help this mutant tolerate alkalinity (Fig. 1). These results are consistent with other studies that have reported that alkalinity-tolerant plants have higher activities of antioxidant enzymes, such as APX, GR, and SOD, and a better GSH redox state (Liu and Saneoka, 2019; Montesinos-Pereira et al., 2018).

4.4. Photosynthesis performance

Several studies showed that alkaline conditions in growth media have a significant impact on photosynthesis (Li et al., 2010, 2014; Roosta, 2011; Wang et al., 2022; Yin et al., 2019). Chl *a* fluorescence and gas exchange analysis are two complementary approaches for analyzing photosynthesis performance and assessing the effects of stress on it (Gurbanova et al., 2019; Strasser et al., 2004). Chl *a* fluorescence measurement is used to study the photochemical stage of photosynthesis and provide various parameters derived from the fluorescence emission (Strasser et al., 2004). The analysis of Chl *a* fluorescence kinetics revealed a negative impact on photosynthetic performance caused by the *BraA.cax1a-7* mutation in the CAX transporter (Fig. 2). Specifically, the results indicate reduced light-harvesting capacity, lower electronic transport between photosystems, and an increase in the waste of potentially useful energy in the form of fluorescence (Strasser et al., 2004). Conversely, the effects of *BraA.cax1a-12* mutation were generally positive. With regard to *BraA.cax1a-4,* its effects were generally negative, although they were not as significant as those caused by *BraA.cax1a-7* (Fig. 2B).

The photosynthetic CO_2 fixation stage and the transpiration rates can be analyzed using an infrared gas analyzer (IRGA) by measuring the CO_2 and H_2O flux in the leaves (Gurbanova et al., 2019). The results obtained by IRGA suggest that *BraA.cax1a-7* had a lower capacity to maintain CO_2 assimilation, while *BraA.cax1a-12* was able to have a good regulation of stomatal aperture and to maintain *A* while avoiding water loss through the stomata (Table 5). Combining the fluorescence and gas exchange results, the *BraA.cax1a-12* variation could be useful for maintaining photosynthetic performance under alkaline conditions and may be related to the better tolerance of this mutant to alkalinity (Table 1). Other studies have shown that the recovery of both fluorescence and gas exchange index values is a good indicator of increased tolerance to alkalinity (Sheoran et al., 2021; Wang et al., 2022; Zhang et al., 2012). Indeed, Wang et al. (2022) observed that Ca^{2+} application enhanced photosynthesis performance and alkalinity tolerance. In our experiment, the changes in photosynthesis due to CAX mutations may be because Ca^{2+} is required for multiple processes within photosynthesis, such as electron flow, protein regulation, stromal signaling, and stomatal response (Hochmal et al., 2015).

5. Conclusions

The application of alkalinity causes stress to *B. rapa* plants, as evidenced by a reduction in biomass, altered nutrient accumulation, oxidative stress, and reduced photosynthetic efficiency. However, the different *BraA.cax1a* variations affected the alkalinity response of *B. rapa*. Thus, *BraA.cax1a-7* had a negative effect on alkalinity tolerance, increased oxidative stress, partially hindered the antioxidant response, and lowered photosynthesis efficiency. Conversely, the *BraA.cax1a-12* mutation improved alkalinity tolerance, which could be related to higher Ca^{2+} accumulation, lower oxidative stress, and better antioxidant response and photosynthesis performance. As for *BraA.cax1a-4*, it showed an intermediate response similar to R-o-18, but enhanced micronutrient accumulation under alkaline conditions. Therefore, in this study, *BraA.cax1a-12* was identified as a useful mutation to improve the performance of plants grown under alkalinity conditions. However, further research is needed to deepen the understanding of the exact mechanisms and to test CAX1 mutations in other species.

Funding

This work was supported by a grant from Plan Propio de Investigación y Transferencia, University of Granada awarded to E.N.L. and by Erasmus traineeship program of the University of Naples "Federico II" awarded to A.G. Funding for open access charge: Universidad de Granada.

Contribution

BB conceived and designed research. ENL, AG, and SAC conducted experiments. ENL, AG and SAC analyzed data. ENL and AG wrote the manuscript. JJR, SE, and BB did a critical revision of the article. All authors read and approved the manuscript.

Declaration of competing interest

The authors declare that they have no known competing financial interests or personal relationships that could have appeared to influence the work reported in this paper.

Data availability

Data will be made available on request.

Acknowledgments

We thank Dr. Martin R. Broadley and Dr. Neil Graham from Nottingham University for providing us the seeds employed in this experiment.

Appendix A. Supplementary data

Supplementary data to this article can be found online at https://doi.org/10.1016/j.plaphy.2023.107712.

References

Ahmadi, H., Corso, M., Weber, M., Verbruggen, N., Clemens, S., 2018. CAX1 suppresses Cd-induced generation of reactive oxygen species in *Arabidopsis halleri*. Plant Cell Environ. 41, 2435–2448. https://doi.org/10.1111/pce.13362.

Bačkor, M., Bačkorová, M., Goga, M., Hrčka, M., 2017. Calcium toxicity and tolerance in lichens: Ca uptake and physiological responses. Water Air Soil Pollut. 228, 56. https://doi.org/10.1007/s11270-017-3239-2.

Bessrour, M., Chelbi, N., Moreno, D.A., Chibani, F., Abdelly, C., Carvajal, M., 2018. Interaction of salinity and $CaCO_3$ affects the physiology and fatty acid metabolism in *Portulaca oleracea*. J. Agric. Food Chem. 66, 6683–6691. https://doi.org/10.1021/acs.jafc.8b01456.

Bradford, M.M., 1976. A rapid and sensitive method for the quantitation of microgram quantities of protein utilizing the principle of protein-dye binding. Anal. Biochem. 72, 248–254. https://doi.org/10.1016/0003-2697(76)90527-3.

Capula-Rodríguez, R., Valdez-Aguilar, L.A., Cartmill, D.L., Cartmill, A.D., Alia-Tejacal, I., 2016. Supplementary calcium and potassium improve the response of tomato (*Solanum lycopersicum* L.) to simultaneous alkalinity, salinity, and boron stress. Commun. Soil Sci. Plant Anal. 1–7. https://doi.org/10.1080/00103624.2016.1141924.

Cardarelli, M., Rouphael, Y., Rea, E., Colla, G., 2010. Mitigation of alkaline stress by arbuscular mycorrhiza in zucchini plants grown under mineral and organic fertilization. J. Plant Nutr. Soil Sci. 173, 778–787. https://doi.org/10.1002/jpln.200900378.

Chakradhar, T., Mahanty, S., Reddy, R.A., Divya, K., Reddy, P.S., Reddy, M.K., 2017. Biotechnological perspective of reactive oxygen species (ROS)-Mediated stress tolerance in plants. In: Reactive Oxygen Species and Antioxidant Systems in Plants: Role and Regulation under Abiotic Stress. Springer Singapore, Singapore, pp. 53–87. https://doi.org/10.1007/978-981-10-5254-5_3.

Conn, S.J., Gilliham, M., Athman, A., Schreiber, A.W., Baumann, U., Moller, I., Cheng, N.-H., Stancombe, M.A., Hirschi, K.D., Webb, A.A.R., Burton, R., Kaiser, B.N., Tyerman, S.D., Leigh, R.A., 2011. Cell-specific vacuolar calcium storage mediated by CAX1 regulates apoplastic calcium concentration, gas exchange, and plant productivity in Arabidopsis. Plant Cell 23, 240–257. https://doi.org/10.1105/tpc.109.072769.

D'Alessandro, A., Taamalli, M., Gevi, F., Timperio, A.M., Zolla, L., Ghnaya, T., 2013. Cadmium stress responses in *Brassica juncea*: hints from proteomics and metabolomics. J. Proteome Res. 12, 4979–4997. https://doi.org/10.1021/pr400793e.

Dayod, M., Tyerman, S.D., Leigh, R.A., Gilliham, M., 2010. Calcium storage in plants and the implications for calcium biofortification. Protoplasma 247, 215–231. https://doi.org/10.1007/s00709-010-0182-0.

de la Torre-González, A., Montesinos-Pereira, D., Romero, L., Blasco, B., Ruiz, J.M., 2018. Analysis of metabolic and nutritional biomarkers in *Brassica oleracea* L. cv. Bronco plants under alkaline stress. J. Hortic. Sci. Biotechnol. 93, 279–288. https://doi.org/10.1080/14620316.2017.1364979.

Derbyshire, M.C., Batley, J., Edwards, D., 2022. Use of multiple 'omics techniques to accelerate the breeding of abiotic stress tolerant crops. Curr Plant Biol 32, 100262. https://doi.org/10.1016/j.cpb.2022.100262.

Fatima, A., Hussain, Saddam, Hussain, Sadam, Ali, B., Ashraf, U., Zulfiqar, U., Aslam, Z., Al-Robai, S.A., Alzahrani, F.O., Hano, C., El-Esawi, M.A., 2021. Differential morphophysiological, biochemical, and molecular responses of maize hybrids to salinity and alkalinity stresses. Agronomy 11, 1150. https://doi.org/10.3390/agronomy11061150.

Fu, J., Huang, B., 2001. Involvement of antioxidants and lipid peroxidation in the adaptation of two cool-season grasses to localized drought stress. Environ. Exp. Bot. 45, 105–114. https://doi.org/10.1016/S0098-8472(00)00084-8.

Graham, N.S., Hammond, J.P., Lysenko, A., Mayes, S., O Lochlainn, S., Blasco, B., Bowen, H.C., Rawlings, C.J., Rios, J.J., Welham, S., Carion, P.W.C., Dupuy, L.X., King, G.J., White, P.J., Broadley, M.R., 2014. Genetical and comparative genomics of Brassica under altered Ca supply identifies Arabidopsis Ca-transporter orthologs. Plant Cell 26, 1–14. https://doi.org/10.1105/tpc.114.128603.

Gurbanova, U.A., Allahverdiyev, T.I., Babayev, H.G., Bayramov, S.M., Huseynova, I.M., 2019. Interaction of photosynthesis, productivity, and environment. In: Photosynthesis, Productivity and Environmental Stress. Wiley, pp. 283–314. https://doi.org/10.1002/9781119501800.ch14.

Gururani, M.A., Venkatesh, J., Tran, L.S.P., 2015. Regulation of photosynthesis during abiotic stress-induced photoinhibition. Mol. Plant 8, 1304–1320. https://doi.org/10.1016/j.molp.2015.05.005.

Hochmal, A.K., Schulze, S., Trompelt, K., Hippler, M., 2015. Calcium-dependent regulation of photosynthesis. Biochim. Biophys. Acta Bioenerg. 1847, 993–1003. https://doi.org/10.1016/J.BBABIO.2015.02.010.

Huang, Y.-M., Wu, Q.-S., 2017. Arbuscular mycorrhizal fungi and tolerance of Fe stress in plants. In: Arbuscular Mycorrhizas and Stress Tolerance of Plants. Springer Singapore, Singapore, pp. 131–145. https://doi.org/10.1007/978-981-10-4115-0_6.

Hunter, M.C., Smith, R.G., Schipanski, M.E., Atwood, L.W., Mortensen, D.A., 2017. Agriculture in 2050: recalibrating targets for sustainable intensification. Bioscience 67, 386–391. https://doi.org/10.1093/biosci/bix010.

Junglee, S., Urban, L., Sallanon, H., Lopez-Lauri, F., 2014. Optimized assay for hydrogen peroxide determination in plant tissue using potassium iodide. Am. J. Anal. Chem. 5, 730–736. https://doi.org/10.4236/ajac.2014.511081.

Law, M.Y., Charles, S.A., Halliwell, B., 1983. Glutathione and ascorbic acid in spinach (*Spinacia oleracea*) chloroplasts. The effect of hydrogen peroxide and of Paraquat. Biochem. J. 210, 899–903. https://doi.org/10.1042/BJ2100899.

Li, R., Shi, F., Fukuda, K., Yang, Y., 2010. Effects of salt and alkali stresses on germination, growth, photosynthesis and ion accumulation in alfalfa (*Medicago sativa* L.). Soil Sci. Plant Nutr. 56, 725–733. https://doi.org/10.1111/j.1747-0765.2010.00506.x.

Li, X., Mu, C., Lin, J., Wang, Y., Li, Y., 2014. Effect of alkaline potassium and sodium salts on growth, photosynthesis, ions absorption and solutes synthesis of wheat seedlings. Exp. Agric. 50, 144–157.

Liu, L., Saneoka, H., 2019. Effects of $NaHCO_3$ acclimation on rye (*secale cereale*) growth under sodic-alkaline stress. Plants 8, 314. https://doi.org/10.3390/plants8090314.

Lochlainn, S.Ó., Amoah, S., Graham, N.S., Alamer, K., Rios, J.J., Kurup, S., Stoute, A., Hammond, J.P., Østergaard, L., King, G.J., White, P.J., Broadley, M.R., 2011. High Resolution Melt (HRM) analysis is an efficient tool to genotype EMS mutants in complex crop genomes. Plant Methods 7, 43. https://doi.org/10.1186/1746-4811-7-43.

Manohar, M., Shigaki, T., Hirschi, K.D., 2011. Plant cation/H^+ exchangers (CAXs): biological functions and genetic manipulations. Plant Biol. 13, 561–569. https://doi.org/10.1111/j.1438-8677.2011.00466.x.

Montesinos-Pereira, D., de la Torre-González, A., Blasco, B., Ruiz, J.M., 2018. Hydrogen sulphide increase the tolerance to alkalinity stress in cabbage plants (*Brassica oleracea* L. 'Bronco'). Sci. Hortic. 235, 349–356. https://doi.org/10.1016/J.SCIENTA.2018.03.021.

Navarro-León, Eloy, López-Moreno, F.J., Atero-Calvo, S., Albacete, A., Ruiz, J.M., Blasco, B., 2020a. CAX1a TILLING mutations modify the hormonal balance controlling growth and ion homeostasis in *Brassica rapa* plants subjected to salinity. Agronomy 10, 1699. https://doi.org/10.3390/agronomy10111699.

Navarro-León, Eloy, López-Moreno, F.J., de la Torre-González, A., Ruiz, J.M., Esposito, S., Blasco, B., 2020b. Study of salt-stress tolerance and defensive mechanisms in *Brassica rapa* CAX1a TILLING mutants. Environ. Exp. Bot. 175, 104061 https://doi.org/10.1016/J.ENVEXPBOT.2020.104061.

Navarro-León, E., Ruiz, J.M., Albacete, A., Blasco, B., 2020. Tolerance to cadmium toxicity and phytoremediation potential of three *Brassica rapa* CAX1a TILLING mutants. Ecotoxicol. Environ. Saf. 189 https://doi.org/10.1016/j.ecoenv.2019.109961.

Navarro-León, E., Ruiz, J.M.J.M., Graham, N., Blasco, B., 2018. Physiological profile of CAX1a TILLING mutants of *Brassica rapa* exposed to different calcium doses. Plant Sci. 272, 164–172.

Noctor, G., Foyer, C.H., 1998. Simultaneous measurement of foliar glutathione, γ-glutamylcysteine, and amino acids by high-performance liquid chromatography: comparison with two other assay methods for glutathione. Anal. Biochem. 264, 98–110. https://doi.org/10.1006/ABIO.1998.2794.

Owino, V., Kumwenda, C., Ekesa, B., Parker, M.E., Ewoldt, L., Roos, N., Lee, W.T., Tome, D., 2022. The impact of climate change on food systems, diet quality, nutrition, and health outcomes: a narrative review. Frontiers in Climate 4. https://doi.org/10.3389/fclim.2022.941842.

Pittman, J.K., Hirschi, K.D., 2016. CAX-ing a wide net: cation/H^+ transporters in metal remediation and abiotic stress signaling. Plant Biol. 18, 741–749. https://doi.org/10.1111/plb.12460.

Rao, M.V., Paliyath, G., Ormrod, D.P., 1996. Ultraviolet-B- and ozone-induced biochemical changes in antioxidant enzymes of Arabidopsis thaliana. Plant Physiol. 110, 125–136. https://doi.org/10.1104/pp.110.1.125.

Roosta, H.R., 2011. Interaction between water alkalinity and nutrient solution ph on the vegetative growth, chlorophyll fluorescence and leaf magnesium, iron, manganese, and zinc concentrations in lettuce. J. Plant Nutr. 34, 717–731. https://doi.org/10.1080/01904167.2011.540687.

Rouphael, Y., Cardarelli, M., di Mattia, E., Tullio, M., Rea, E., Colla, G., 2010. Enhancement of alkalinity tolerance in two cucumber genotypes inoculated with an arbuscular mycorrhizal biofertilizer containing Glomus intraradices. Biol. Fertil. Soils 46, 499–509. https://doi.org/10.1007/s00374-010-0457-9.

Sheoran, P., Basak, N., Kumar, A., Yadav, R.K., Singh, R., Sharma, R., Kumar, S., Singh, R.K., Sharma, P.C., 2021. Ameliorants and salt tolerant varieties improve rice-wheat production in soils undergoing sodification with alkali water irrigation in Indo–Gangetic Plains of India. Agric. Water Manag. 243, 106492 https://doi.org/10.1016/J.AGWAT.2020.106492.

Soloklui, A.A.G., Ershadi, A., Fallahi, E., 2012. Evaluation of cold hardiness in seven Iranian commercial pomegranate (*Punica granatum* L.) cultivars. Hortscience 47 (12), 1821–1825.

Strasser, R., Srivastava, A., Tsimilli-Michael, M., 2000. The fluorescence transient as a tool to characterize and screen photosynthetic samples. In: Yunus, M., Pathre, U., Mohanty, P. (Eds.), Probing Photosynthesis: Mechanism, Regulation and Adaptation. Taylor & Francis, London, pp. 443–480.

Strasser, R.J., Tsimilli-Michael, M., Srivastava, A., 2004. Analysis of the chlorophyll a fluorescence transient. In: Chlorophyll a Fluorescence. Springer Netherlands, Dordrecht, pp. 321–362. https://doi.org/10.1007/978-1-4020-3218-9_12.

Taalab, A., Ageeb, G., Siam, H., Mahmoud, S., 2019. Some characteristics of calcareous soils. A review. Middle East Journal of Agriculture Research 8, 96–105.

Tamir, G., Zilkah, S., Dai, N., Shawahna, R., Cohen, S., Bar-Tal, A., 2021. Combined effects of $CaCO_3$ and the proportion of N-NH_4^+ among the total applied inorganic N on the growth and mineral uptake of rabbiteye blueberry. J. Soil Sci. Plant Nutr. 21, 35–48. https://doi.org/10.1007/s42729-020-00339-2.

Till, B.J., Datta, S., Jankowicz-Cieslak, J., 2018. TILLING: the Next Generation. Springer, Cham, pp. 139–160. https://doi.org/10.1007/10_2017_54.

Uzuner, Ç., Dengiz, O., 2020. Desertification risk assessment in Turkey based on environmentally sensitive areas. Ecol. Indicat. 114, 106295 https://doi.org/10.1016/J.ECOLIND.2020.106295.

Valdez-Aguilar, L.A., Reed, D.Wm, 2007. Response of selected greenhouse ornamental plants to alkalinity in irrigation water. J. Plant Nutr. 30, 441–452. https://doi.org/10.1080/01904160601171983.

Wang, S., Leus, L., Lootens, P., van Huylenbroeck, J., van Labeke, M.-C., 2022. Germination kinetics and chlorophyll fluorescence imaging allow for early detection of alkalinity stress in Rhododendron species. Horticulturae 8, 823. https://doi.org/10.3390/horticulturae8090823.

Wei, T.-J., Jiang, C.-J., Jin, Y.-Y., Zhang, G.-H., Wang, M.-M., Liang, Z.-W., 2020. Ca^{2+}/Na^+ ratio as a critical marker for field evaluation of saline-alkaline tolerance in alfalfa (*Medicago sativa* L.). Agronomy 10, 191. https://doi.org/10.3390/agronomy10020191.

White, P.J., Broadley, M.R., 2003. Calcium in plants. Ann. Bot. 92, 487–511. https://doi.org/10.1093/aob/mcg164.

Wolf, B., 1982. A comprehensive system of leaf analyses and its use for diagnosing crop nutrient status. Commun. Soil Sci. Plant Anal. 13, 1035–1059. https://doi.org/10.1080/00103628209367332.

Xiao, H., He, W., Fu, W., Cao, H., Fan, Z., 1999. A spectrophotometer method testing oxygen radicals. Prog. Biochem. Biophys. 26, 180–182.

Yin, Z., Zhang, H., Zhao, Q., Yoo, M.-J., Zhu, N., Yu, Jianlan, Juanjuan, Yu, Guo, S., Miao, Y., Chen, S., Qin, Z., Dai, S., 2019. Physiological and comparative proteomic analyses of saline-alkali $NaHCO_3$-responses in leaves of halophyte *Puccinellia tenuiflora*. Plant Soil 437, 137–158. https://doi.org/10.1007/s11104-019-03955-9.

Yu, Q., Osborne, L., Rengel, Z., 1998. Micronutrient deficiency changes activities of superoxide dismutase and ascorbate peroxidase in tobacco plants. J. Plant Nutr. 21, 1427–1437. https://doi.org/10.1080/01904169809365493.

Zhang, X.W., Dong, Y.J., Qiu, X.K., Hu, G.Q., Wang, Y.H., Wang, Q.H., 2012. Exogenous nitric oxide alleviates iron-deficiency chlorosis in peanut growing on calcareous soil. Plant Soil Environ. 58, 111–120.